Microstrip Antennas- Rectangular Patch

Chapter 14 in *Antenna Theory, Analysis and Design* (4th Edition) by Balanis

Cavity model

- Microstrip antennas resemble dielectric-loaded cavities that are bounded by electrical conductors on the top & bottom (i.e., tangential electric fields are zero) and magnetic walls (i.e., tangential magnetic fields are zero) on the sides.

- A pure cavity model does not account for the part of the field that is radiated. Radiation loss is worked into the model by introducing an effective loss tangent $\delta_{eff} = 1/Q$ where Q is the antenna quality factor.

- Since $h << \lambda$, the electric field is nearly normal to the patch (neglect fringing) inside the cavity, i.e., the electric field is in the x-direction. This leads us to consider only the transverse magnetic (TM^x) field configurations or modes.

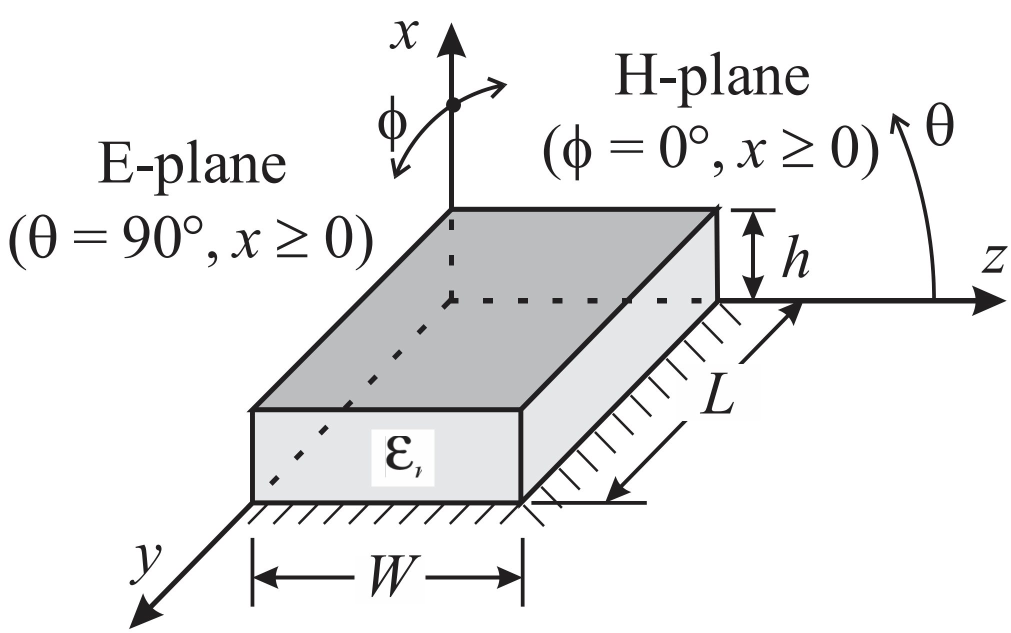

Rectangular microstrip patch geometry.

TM^x field configurations or modes

The wave equation that will be solved, for the dielectric cavity is

$$\nabla^2 A_x + k^2 A_x = 0$$

where A_x is the x-component of the vector magnetic potential and k is the wave number. The general solution for A_x is

$$A_x = \left[A_1 \cos(k_x x) + B_1 \sin(k_x x)\right]\left[A_2 \cos(k_y y) + B_2 \sin(k_y y)\right]$$
$$\times\left[A_3 \cos(k_z z) + B_3 \sin(k_z z)\right]$$

where k_x, k_y, and k_z are the wave numbers in the indicated directions.

The applicable boundary conditions are:

a) Top and Bottom of cavity (electrical conductors)

$$E_y(x' = 0, 0 \le y' \le L, 0 \le z' \le W) = E_y(x' = h, 0 \le y' \le L, 0 \le z' \le W) = 0$$

b) Sides of cavity (magnetic walls)

$$H_y(0 \le x' \le h, 0 \le y' \le L, z' = 0) = H_y(0 \le x' \le h, 0 \le y' \le L, z' = W) = 0$$

$$H_z(0 \le x' \le h, y' = 0, 0 \le z' \le W) = H_z(0 \le x' \le h, y' = L, 0 \le z' \le W) = 0$$

where the primed coordinates represent the inside of the cavity.

Applying these boundary conditions leads to

$$A_x = A_{mnp} \cos(k_x x') \cos(k_y y') \cos(k_z z')$$

where A_{mnp} is the product of the amplitude coefficients and the wave numbers are

$$\left.\begin{aligned} k_x &= \frac{m\pi}{h} \quad m = 0,1,2,\ldots \\ k_y &= \frac{n\pi}{L} \quad n = 0,1,2,\ldots \\ k_z &= \frac{p\pi}{W} \quad p = 0,1,2,\ldots \end{aligned}\right\} \begin{array}{c} m = n = p \neq 0 \\ \text{(can't all be zero)} \end{array}$$

and

$$k_x^{\;2} + k_y^{\;2} + k_z^{\;2} = k_r^{\;2} = \omega_r^{\;2}\mu\varepsilon\,.$$

The subscript *r* refers to the resonant frequency.

The resonant frequency is

$$\left(f_r\right)_{mnp} = \frac{1}{2\pi\sqrt{\mu\varepsilon}}\sqrt{\left(\frac{m\pi}{h}\right)^2 + \left(\frac{n\pi}{L}\right)^2 + \left(\frac{p\pi}{W}\right)^2}\;.$$

After solving for A_x, the electric and magnetic fields can be found from the vector magnetic potential using

$$\begin{aligned} E_x &= -j\frac{1}{\omega\mu\varepsilon}\left(\frac{\partial A_x}{\partial x^2} + k^2 A_x\right) \\ E_y &= -j\frac{1}{\omega\mu\varepsilon}\frac{\partial^2 A_x}{\partial x \partial y} \\ E_z &= -j\frac{1}{\omega\mu\varepsilon}\frac{\partial^2 A_x}{\partial x \partial z} \end{aligned}$$

and

$$H_x = 0 \quad \text{(transverse magnetic)}$$

$$H_y = \frac{1}{\mu}\frac{\partial A_x}{\partial z}$$

$$H_z = \frac{1}{\mu}\frac{\partial A_x}{\partial y}$$

which yields

$$E_x = -j\frac{k^2 - k_x^{\,2}}{\omega\mu\varepsilon} A_{mnp} \cos(k_x x')\cos(k_y y')\cos(k_z z')$$

$$E_y = -j\frac{k_x k_y}{\omega\mu\varepsilon} A_{mnp} \sin(k_x x')\sin(k_y y')\cos(k_z z')$$

$$E_z = -j\frac{k_x k_z}{\omega\mu\varepsilon} A_{mnp} \sin(k_x x')\cos(k_y y')\sin(k_z z')$$

and

$$H_x = 0$$

$$H_y = -\frac{k_z}{\mu} A_{mnp} \cos(k_x x')\cos(k_y y')\sin(k_z z')$$

$$H_z = \frac{k_y}{\mu} A_{mnp} \cos(k_x x')\sin(k_y y')\cos(k_z z')$$

The electric field configurations for the lowest few cavity modes are shown in Figure 14.13.

The dominant mode (i.e., the mode with the lowest resonant frequency) depends on the dimensions of the cavity (patch). Since the cavity height (substrate thickness) is much smaller than the length and width of the patch, i.e., $h << L$ and $h << W$, the length L and width W of the patch will control the dominant mode.

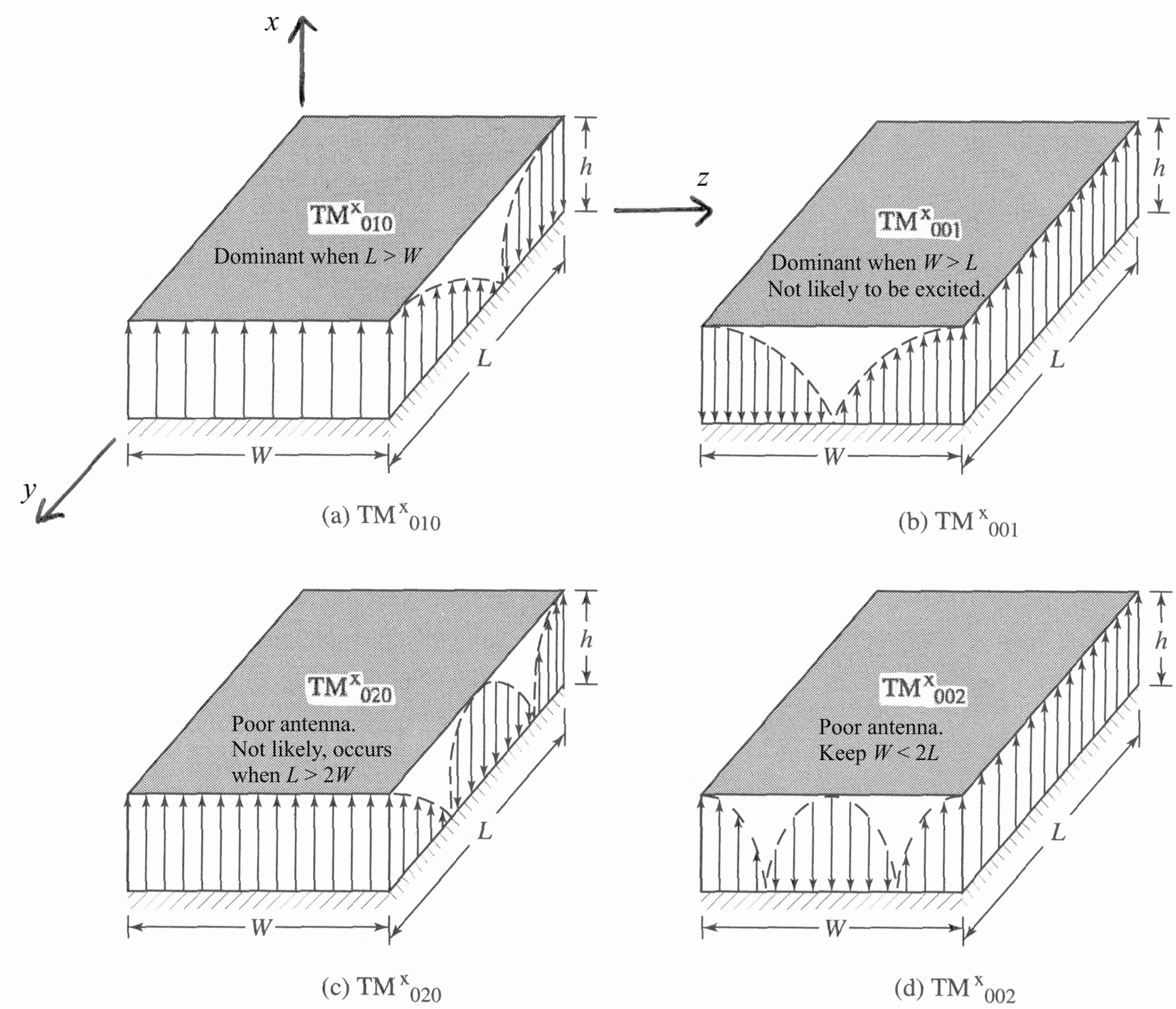

Figure 14.16 Field configurations (modes) for rectangular microstrip patch. [From Balanis, *Antenna Theory, Analysis and Design (Fourth Edition)*]

If $L > W > h$, the dominant mode (and desired mode) is the $TM^x{}_{010}$ where the resonant frequency is

$$\left(f_r\right)_{010} = \frac{1}{2L\sqrt{\mu\varepsilon}} = \frac{c}{2L\sqrt{\varepsilon_r}}.$$

Further, if $L > W > L/2 > h$, the next highest mode (after $TM^x{}_{010}$) is the $TM^x{}_{001}$

$$\left(f_r\right)_{001} = \frac{1}{2W\sqrt{\mu\varepsilon}} = \frac{c}{2W\sqrt{\varepsilon_r}}.$$

However, if $W > L > h$, the <u>dominant mode</u> is the TM^x_{001} whose resonant frequency has already been given. Fortunately, if a centered microstrip feed is used, the TM^x_{010} mode can be excited, even if it is not the dominant mode (see Fig 14.13a).

If $L > L/2 > W > h$, the dominant mode would be the TM^x_{020}

$$\left(f_r\right)_{020} = \frac{1}{L\sqrt{\mu\varepsilon}} = \frac{c}{L\sqrt{\varepsilon_r}} \ .$$

If $W > W/2 > L > h$, the next highest mode (after TM^x_{001}) is the TM^x_{002}

$$\left(f_r\right)_{002} = \frac{1}{2W\sqrt{\mu\varepsilon}} = \frac{c}{2W\sqrt{\varepsilon_r}} \ .$$

Note: These calculations ignore the effects of fringing and assume that the dielectric substrate is only under the patch.

<u>Radiation</u> (TM^x_{010} mode)

Assuming the active or dominant mode is the TM^x_{010}, the fields in the cavity are

$$E_x = E_0 \cos\left(\frac{\pi}{L} y'\right) \text{ and } H_z = H_0 \sin\left(\frac{\pi}{L} y'\right)$$
$$E_y = E_z = H_x = H_y = 0$$

where $n = 1$, $m = p = 0$, $E_0 = -j\omega A_{010}$, and $H_0 = (\pi/\mu L)\, A_{010}$. See Figure 14.13a for pictures of the electric field distribution. Radiation occurs from the two end slots (located at $y = 0$ and $y = L$). The rectangular slots have dimensions of $W \times h$, and are separated by about $\lambda/2$ at resonance. The side slots (located at $z = 0$ and $z = W$) are non-radiating because the radiation from the fields along the sides cancel each other in the far-field (note that along half the side slots the electric field points up and on the other half it points down).

The far-field radiated electric fields radiated by each slot by itself (see Chapter 12) are

$$E_r \approx E_\theta \approx 0$$

$$E_\phi = j\frac{k_0 h W E_0 e^{-jk_0 r}}{2\pi r}\left[\sin\theta\frac{\sin(X)}{X}\frac{\sin(Z)}{Z}\right]$$

where θ and ϕ are the standard spherical coordinate angles, and

$$X = \frac{k_0 h}{2}\sin\theta\cos\phi$$

$$Z = \frac{k_0 W}{2}\cos\theta$$

If $k_0 h << 1$, then E_ϕ reduces to

$$E_\phi = j\frac{hE_0 e^{-jk_0 r}}{\pi r}\left[\sin\theta\frac{\sin\left(\frac{k_0 W}{2}\cos\theta\right)}{\cos\theta}\right]$$

Note, the voltage across the slot is $V_0 = hE_0$.

Modeling the two radiating slots as a two-element array (see Chapter 6) of rectangular aperture antennas leads to

$$E_r \approx E_\theta \approx 0$$

$$E_\phi^{\text{tot}} = j\frac{k_0 h W E_0 e^{-jk_0 r}}{\pi r}\left[\sin\theta\frac{\sin(X)}{X}\frac{\sin(Z)}{Z}\right]\cos\left(\frac{k_0 L_{\text{eff}}}{2}\sin\theta\sin\phi\right).$$

Again, if $k_0 h << 1$, this reduces to

$$E_\phi^{\text{tot}} = j\frac{2hE_0 e^{-jk_0 r}}{\pi r}\left[\sin\theta\frac{\sin\left(\frac{k_0 W}{2}\cos\theta\right)}{\cos\theta}\right]\cos\left(\frac{k_0 L_{\text{eff}}}{2}\sin\theta\sin\phi\right).$$

Note, the voltage across the slot is $V_0 = hE_0$.

The radiated electrical field in the two principal planes are-

***E*-plane**

$$E_\phi^{\text{tot}} = j\frac{k_0 W h E_0 e^{-jk_0 r}}{\pi r}\left[\frac{\sin\left(\frac{k_0 h}{2}\cos\phi\right)}{\frac{k_0 h}{2}\cos\phi}\right]\cos\left(\frac{k_0 L_{\text{eff}}}{2}\sin\phi\right)$$

on the *x*-*y* plane above the ground where θ = 90° = π/2 and 0 ≤ ϕ ≤ 90° & 270° ≤ ϕ < 360°, and

***H*-plane**

$$E_\phi^{\text{tot}} = j\frac{k_0 W h E_0 e^{-jk_0 r}}{\pi r}\left[\sin\theta\frac{\sin\left(\frac{k_0 h}{2}\sin\theta\right)}{\frac{k_0 h}{2}\sin\theta}\frac{\sin\left(\frac{k_0 W}{2}\cos\theta\right)}{\frac{k_0 W}{2}\cos\theta}\right]$$

on the *x*-*z* plane above the ground where, ϕ = 0 and 0 ≤ θ ≤ 180°.

Figure 14.18 shows examples of typical *E*-plane and *H*-plane radiation patterns. Note that the experimental, theoretical, and MoM results agree well on the *H*-plane. However, there are some differences in the results at low angles (near the dielectric substrate) between the different methods for the *E*-plane. This is primarily because the cavity theory assumed the dielectric substrate was truncated at the edges of the cavity, which does not happen in reality. Also, the experimental results differ from the cavity model and MoM results due to the reality of using a finite ground which allows the fields to get below the *x*-*y* plane ($z < 0$).

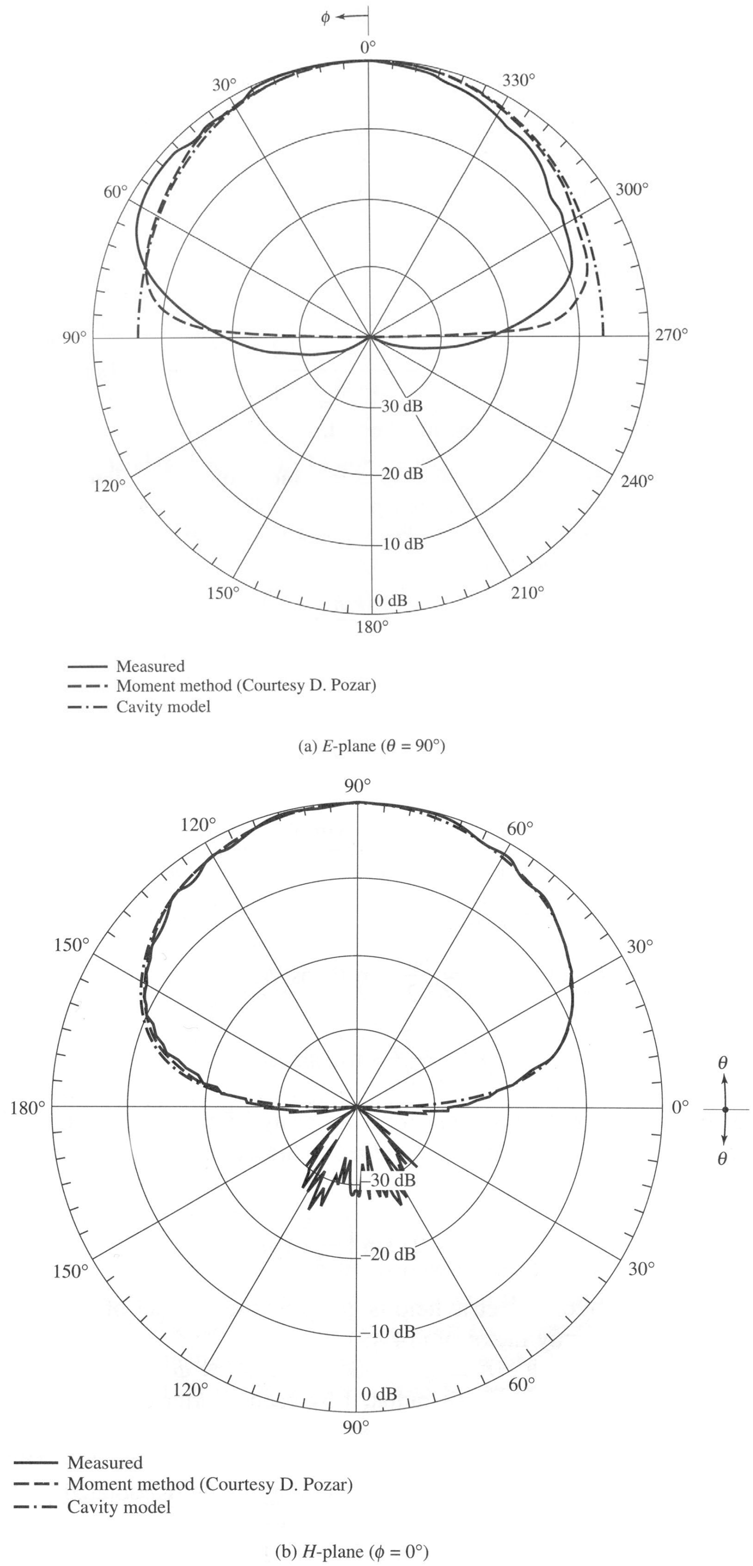

Figure 14.18 Predicted and measured E- and H-plane patterns of rectangular microstrip patch ($L = 0.906$cm, $W = 1.186$ cm, $y_0 = 0.3126$ cm, $\varepsilon_r = 2.2$, $f_0 = 10$GHz). [From Balanis, *Antenna Theory, Analysis & Design* (*Second Edition*)]

Directivity

Knowing the fields allows the directivity of the rectangular patch to be calculated. In particular, we are interested in the maximum directivity

$$D_{\max} = D_0 = \frac{U_{\max}}{U_0} = \frac{4\pi U_{\max}}{P_{\text{rad}}}.$$

For the typical case that $k_0 h \ll 1$, the maximum radiation intensity and the power radiated by a <u>single rectangular slot</u> are

$$U_{\max} = \frac{|V_0|^2}{2\eta_0 \pi^2} \left(\frac{\pi W}{\lambda_0} \right)^2$$

and

$$P_{\text{rad}} = \frac{|V_0|^2}{2\eta_0 \pi^2} \int_{\theta=0}^{\pi} \left[\frac{\sin\left(\frac{k_0 W}{2} \cos\theta \right)}{\cos\theta} \right]^2 \sin^3\theta \, d\theta .$$

The maximum directivity of a **single** rectangular slot is then

$$D_{\max} = D_0 = \left(\frac{2\pi W}{\lambda_0} \right)^2 \frac{1}{I_1}$$

where I_1 is

$$\begin{aligned} I_1 &= \int_{\theta=0}^{\pi} \left[\frac{\sin\left(\frac{k_0 W}{2} \cos\theta \right)}{\cos\theta} \right]^2 \sin^3\theta \, d\theta \\ &= -2 + \cos(k_0 W) + k_0 W \, S_i(k_0 W) + \frac{\sin(k_0 W)}{k_0 W} \end{aligned}$$

The maximum directivity of a single slot is shown in Figure 14.22.

The maximum directivity of a rectangular patch (2 radiating slots) is

$$D_{\max}^{\text{tot}} = D_0^{\text{tot}} = \left(\frac{2\pi W}{\lambda_0}\right)^2 \frac{\pi}{I_2} = \frac{2}{15G_{\text{rad}}}\left(\frac{W}{\lambda_0}\right)$$

where G_{rad} is the radiation conductance and the parameter

$$I_2 = \int_{\phi=0}^{\pi}\int_{\theta=0}^{\pi}\left[\frac{\sin\left(\dfrac{k_0 W}{2}\cos\theta\right)}{\cos\theta}\right]^2 \sin^3\theta\cos^2\left(\frac{k_0 L_{\text{eff}}}{2}\sin\theta\sin\phi\right)d\theta\, d\phi\,.$$

An alternate expression for calculating the maximum directivity of a rectangular patch (2 radiating slots), using the single slot result, is

$$D_{\max}^{\text{tot}} = D_0^{\text{tot}} = D_0\left(\frac{2}{1+G_{12}/G_1}\right)$$

where D_0 is the directivity of a single slot, G_1 is the slot conductance, and G_{12} is the mutual conductance between the slots.

The directivities for two slots (i.e., rectangular patch) are shown in Figures 14.22 and 14.23 as functions of slot width W and substrate height h.

The HPBWs in the E-plane and H-planes are (very) approximately

$$\Theta_E \simeq 2\sin^{-1}\sqrt{\frac{7.03\lambda_0^{\;2}}{4\pi^2\left(3L_{\text{eff}}^{\;2}+h^2\right)}} \qquad (14\text{-}58)$$

and

$$\Theta_H \simeq 2\sin^{-1}\sqrt{\frac{1}{2+k_0 W}} \qquad (14\text{-}59)\,.$$

To get accurate HPBWs, use the expressions for $E_\phi^{\;\text{tot}}$ in the E- and H-planes to find where $\left|E_\phi^{\;\text{tot}}\right| = \left|E_{\phi,\max}^{\;\;\text{tot}}\right|/\sqrt{2} = 0.707\left|E_{\phi,\max}^{\;\;\text{tot}}\right|$ with respect to θ or ϕ as applicable.

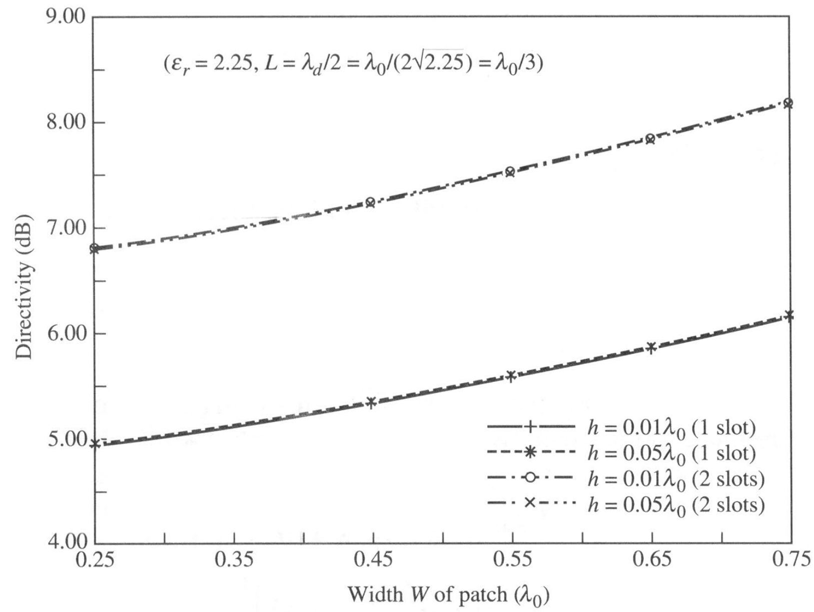

Figure 14.22 Computed directivity of one and two slots as a function of the slot width. [From Balanis, *Antenna Theory, Analysis and Design (Fourth Edition)*]

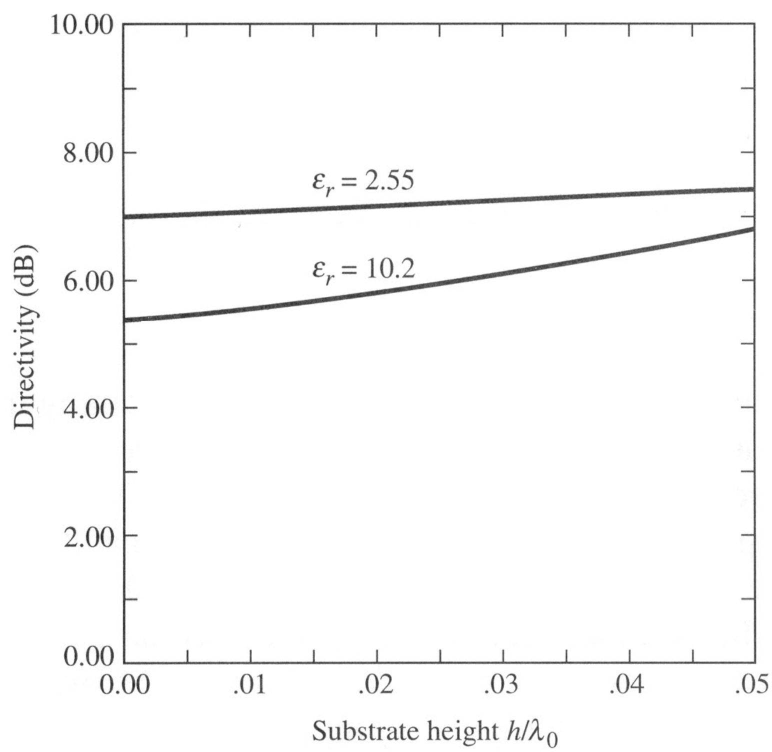

Figure 14.23 Directivity variations as a function of substrate height for a square microstrip patch antenna (courtesy of D. M. Pozar). [From Balanis, *Antenna Theory, Analysis and Design (Fourth Edition)*]